Chapter 5
Operational Modal Analysis of Rotating Structures Under Ambient Excitation Using Tracking Continuously Scanning Laser Doppler Vibrometry

L. F. Lyu and W. D. Zhu

Abstract A continuously scanning laser Doppler vibrometer (CSLDV) system is capable of rapidly obtaining spatially dense vibration measurement by continuously sweeping its laser spot along a path on a structure surface. This paper presents a new operational modal analysis (OMA) method for a rotating structure based on a rigorous rotating beam vibration theory, an image processing method, and a data processing method called the lifting method. A novel tracking CSLDV (TCSLDV) system was developed in this work to track and scan a rotating structure, and the real-time position of the rotating structure can be determined by image processing so that the TCSLDV system is capable of tracking a time-varying scan path on the rotating structure. The lifting method can transform raw TCSLDV measurement into measurements at multiple virtual measurement points as if they were measured by transducers attached to these measurement points. Modal parameters of the rotating structure with a constant speed, including damped natural frequencies, undamped mode shapes, and modal damping ratios, and operating deflection shapes (ODSs) of the structure with a constant or prescribed time-varying rotation speed can be determined by calculating and analyzing correlation functions with non-negative time delays among measurements at virtual measurement points. Experimental investigation is conducted using the TCSLDV system to study the OMA method with which modal parameters and an ODS of a rotating fan blade with different constant speeds, as well as an ODS of the rotating fan blade with a non-constant speed, are successfully estimated.

Keywords Tracking continuously scanning laser Doppler vibrometer system · Rotating beam vibration theory · Operational modal analysis · Lifting method · Operating deflection shapes

5.1 Introduction

Modal analysis studies modal parameters such as natural frequencies, mode shapes, and modal damping ratios of a linear structure [1]. Modal analysis methods can be divided into experimental modal analysis (EMA) methods and operational modal analysis (OMA) methods, depending on whether an excitation applied on the structure needs to be measured or not [2]. An EMA method requires excitation measurement, while an OMA method does not. Frequency response functions or impulse response functions of the structure are calculated and analyzed to estimate its modal parameters in EMA methods [1]. Correlation functions with non-negative time delays and their power spectra are calculated and analyzed to estimate modal parameters in OMA methods based on the natural excitation testing theory [3, 4]. Siringoringo and Fujino [5] proposed and investigated a time-synchronization technique to calculate correlation functions for simultaneously estimating modal parameters in OMA methods. Compared with EMA methods, modal parameters can be accurately estimated in OMA methods when the structure is assumed to be under white-noise excitation that is unknown or not measured. Hence OMA methods are more appropriate for structures under operating conditions or under ambient excitations.

A laser Doppler vibrometer that is considered to be one of the most accurate and reliable vibration measurement tools can measure the surface velocity of a point on a structure along its laser beam direction [6]. However, the measurement efficiency of a laser vibrometer becomes critical when there is a large and dense measurement grid. A laser vibrometer can be equipped with a scanner that has a set of orthogonal mirrors to increase its measurement efficiency [7]. The laser spot of the vibrometer is able to continuously sweep along a prescribed path on a structure to measure its surface velocity by rotating the mirrors that are controlled by a controller. When rotation angles of the mirrors continuously change, since the path and speed of the

L. F. Lyu · W. D. Zhu (✉)
Department of Mechanical Engineering, University of Maryland, Baltimore, MD, USA
e-mail: linfenl1@umbc.edu; wzhu@umbc.edu

D. Di Maio, J. Baqersad (eds.), *Rotating Machinery, Optical Methods & Scanning LDV Methods, Volume 6*, Conference Proceedings of the Society for Experimental Mechanics Series, https://doi.org/10.1007/978-3-030-76335-0_5

laser spot on the structure can be controlled, various scans of the laser spot can be created. The laser vibrometer, scanner, and controller of the scanner constitute a continuous scanning laser Doppler vibrometer (CSLDV) system [7–9]. When the sampling frequency of the CSLDV system is high, the system can efficiently perform spatially dense vibration measurement.

To analyze CSLDV measurements of structures undergoing different vibrations such as sinusoidal vibration, free vibration, and random vibration, various methods have been proposed. One method is the demodulation method [8, 10] for a structure undergoing sinusoidal vibration. The polynomial method [8, 10] is another method for a structure undergoing sinusoidal vibration, where real and imaginary parts of the ODS are represented by two polynomials. The demodulation method was later applied to identify damage in beams and plates undergoing sinusoidal vibration [11, 12]. Based on the demodulation method, Xu et al. [13] introduced a free response shape, which is a new type of vibration shapes. The free response shape corresponding to one mode of a structure can be used for baseline-free damage identification of the structure. A lifting method converts CSLDV measurement of a structure undergoing free vibration into measurements at multiple virtual measurement points as if there were transducers attached to these points for EMA [9]. An OMA method for a structure under ambient excitation was developed with a CSLDV system in Ref. [14], where harmonic transfer functions and harmonic power spectra [15] were employed. An OMA method that combines the lifting method and harmonic transfer functions was proposed in Ref. [16], where processing and interpretation of CSLDV measurement become simpler. Xu et al. [17] proposed a new OMA method for CSLDV measurement based on the lifting method to estimate modal parameters of damaged structures and detect local anomaly caused by damage on a scan path.

To estimate modal parameters of a rotating structure, encoders were used to track its angular position [18, 19]. Khalil et al. [18] proposed a method to track a rotating structure and measure its ODSs by attaching an encoder to it. Allen et al. [19] developed an EMA method to measure mode shapes of a rotating fan with an encoder attached to its shaft to track its angular position. However, it is difficult to attach an encoder to a rotating structure such as a large horizontal-axis wind turbine; a more convenient OMA method and CSLDV system for tracking the angular position of a rotating structure and estimating its modal parameters and ODSs are needed.

In this work, a new OMA method based on a rotating beam vibration theory, an image processing method, and the modal parameter estimation method in Ref. [17] is developed to estimate the rotation speed, modal parameters, and ODSs of a rotating structure under ambient excitation. A camera is used to capture images of the rotating structure so that a CSLDV system can track the structure by processing its images. Raw CSLDV measurement is transformed into measurements at multiple virtual measurement points using the lifting method. The OMA method can be used to estimate modal parameters of the rotating structure with a constant speed, including damped natural frequencies, undamped mode shapes, and modal damping ratios, by calculating and analyzing correlation functions between lifted measurements at virtual measurement points and a reference measurement point and their power spectra. It can also be used to estimate ODSs of the rotating structure with a constant or prescribed time-varying speed.

Experimental investigation of the OMA method was conducted on a rotating fan blade under ambient excitation using a new tracking CSLDV (TCSLDV) system that consists of a laser vibrometer, a scanner with its controller, and a camera. The fan was vertically mounted on a stationary frame, which can be considered as a model of a wind turbine. Modal parameters and the ODS of the fan blade with a constant rotation speed and the ODS of the fan blade with a non-constant rotation speed were estimated.

5.2 Methodology

As shown in Fig. 5.1, consider a fan blade that rotates about the z axis, which, without loss of generality, can be modeled as a uniform, rotating Euler-Bernoulli beam with a length l attached to a rigid hub with a radius b. Two coordinate systems are considered: an inertial coordinate system O-XYZ and a rotating coordinate system o-xyz whose origin o is at the center of the rigid hub, which is referred to as the rotation center; the z axis is parallel to the Z axis. The position of the origin O of the inertial coordinate system O-XYZ depends on the position of the camera of the TCSLDV system. Small transverse vibration of the beam along the z axis is considered and vibrations along x and y axes are neglected. The x axis passes through the rotation center and is tangent to the neutral axis of the beam at the point where the beam is attached to the hub. Assume that the beam has linear viscous damping in the z direction.

By following Refs. [20, 21], the governing equation of the uniform rotating Euler-Bernoulli beam under a distributed, external white-noise excitation force $f(x, t)$ in the z direction and its associated boundary conditions are derived using the extended Hamilton's principle:

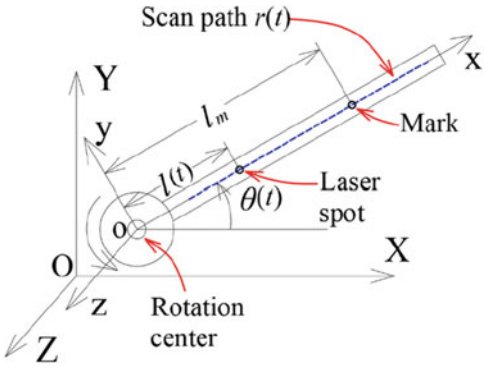

Fig. 5.1 Schematic of a rotating structure

$$\begin{aligned}&\rho w_{tt}(x,t)+C\left[w_t(x,t)\right]+EIw_{xxxx}(x,t)\\&-\tfrac{1}{2}\rho\dot{\theta}^2(t)\left[\left((b+l)^2-x^2\right)w_{xx}(x,t)-2xw_x(x,t)\right]=f(x,t),\ b\le x\le b+l,\ t>0\end{aligned}\tag{5.1}$$

$$w(x,t)|_{x=b}=w_x(x,t)|_{x=b}=w_{xx}(x,t)|_{x=b+l}=w_{xxx}(x,t)|_{x=b+l}=0\tag{5.2}$$

where the subscripts denote partial differentiation; an overdot denotes a time derivative; x is the spatial position along the x axis; t is time; $\theta(t)$ is the angle between x- and X-axes, as shown Fig. 5.1; w is the transverse displacement of the beam at the position x and time t along the z axis; ρ and EI are the mass per unit length and flexural rigidity of the beam, respectively; and $C(\cdot)$ is the damping operator. Note that Eqs. (5.1) and (5.2) are applicable to a rotating beam with a prescribed time-varying speed $\dot{\theta}(t)$. When $\dot{\theta}(t)=\Omega$ is a constant, assume that the rotating beam is under a concentrated force $f_a(t)$ applied at x_a; the solution to Eqs. (5.1) and (5.2) can be written as

$$w(x,t)=\sum_{i=1}^{\infty}\phi_i(x)\phi_i(x_a)\int_0^t f_a(\tau)\,g_i(t-\tau)\,\mathrm{d}\tau\tag{5.3}$$

where $\phi_i(x)$ is the i-th undamped mode shape of the rotating beam and $g_i(t)$ is the unit impulse response function of the beam corresponding to its i-th underdamped mode:

$$g_i(t)=\frac{1}{\omega_{d,i}}\mathrm{e}^{-\zeta_i\omega_i t}\sin\left(\omega_{d,i}t\right)\tag{5.4}$$

where ω_i, ζ_i, and $\omega_{d,i}=\omega_i\sqrt{1-\zeta_i^2}$ are the i-th real undamped natural frequency, modal damping ratio, and damped natural frequency of the rotating beam, respectively. Virtual measurement points are assigned on the fan blade in Fig. 5.1 along a time-varying scan path $r(t)$ when the TCSLDV system is used to periodically measure w by scanning its laser spot along the path $r(t)$. The TCSLDV system registers discrete measurements of w with a finite sampling frequency F_{sa}.

A scan path $r(t)$ is usually a straight line on a rotating structure, which is the case considered here. If a CSLDV system is used to scan along a stationary structure and positions of the laser spot can be considered to be linearly related to the rotation angle of a mirror (e.g., X-mirror) in the scanner in the CSLDV, only the X-mirror is needed to complete the scan, and the mirror signal can be directly used as the position of the laser spot on the scan path $r(t)$. However, both X- and Y-mirrors are needed to scan along a rotating structure such as the fan blade here; thus use of only one mirror signal is not enough to describe the position of the laser spot on the scan path $r(t)$. A simulated X-mirror signal for scanning a stationary structure is shown in Fig. 5.2a. Simulated X- and Y-mirror signals for scanning a rotating structure with a constant speed are shown in Fig. 5.2b. A new method is developed in this work to combine X- and Y-mirror signals to describe the position of a laser spot on the scan path $r(t)$ on a rotating structure.

A mark is attached to a structure that rotates with a constant speed to identify positions of the structure and scan path at any time instant (Fig. 5.1). Let the position of the rotation center relative to the inertial coordinate system XYZ be (u_0, v_0), the position of the mark be $(u_m(t), v_m(t))$, and the position of the laser spot be $(u(t), v(t))$; one has

$$\begin{cases}u_m(t)-u_0=l_m\cos(\theta(t))=l_m\cos(\Omega t)\\ v_m(t)-v_0=l_m\sin(\theta(t))=l_m\sin(\Omega t)\end{cases},\tag{5.5}$$

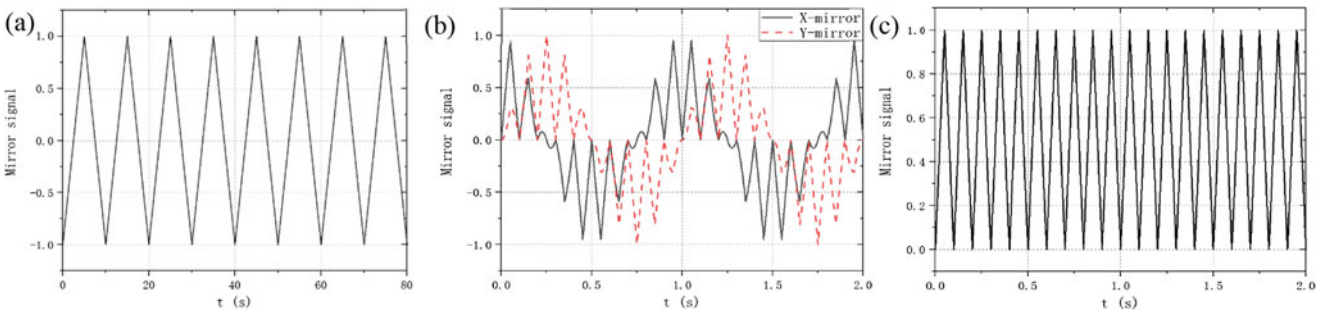

Fig. 5.2 Simulated mirror signals of a CSLDV system: (**a**) the X-mirror signal for scanning a stationary structure; (**b**) X- and Y-mirror signals for scanning a rotating structure; and (**c**) the processed mirror signal by combining mirror signals in (**b**)

$$\begin{cases} u(t) - u_0 = l(t)\cos(\theta(t)) = l(t)\cos(\Omega t) \\ v(t) - v_0 = l(t)\sin(\theta(t)) = l(t)\sin(\Omega t) \end{cases}, \tag{5.6}$$

where l_{m} is the distance between the rotation center and mark and $l(t)$ is the distance between the rotation center and laser spot at time t, which can be used to describe the position of the laser spot on the scan path $r(t)$. Since the scan path lies on a straight line through the rotation center, the distance between the rotation center and laser spot is

$$r(t) = \sqrt{(u(t) - u_0)^2 + (v(t) - v_0)^2} \tag{5.7}$$

where u and v are X- and Y-mirror signals, respectively. The position of the laser spot on the scan path $r(t)$ can be obtained by combining X- and Y-mirror signals using Eq. (5.7). The processed mirror signal by this method is shown in Fig. 5.2c. The method can also be applied to a structure that rotates with a prescribed time-varying speed. The solution w in Eq. (5.3) can be written as a function of $l(t)$ and t:

$$w[l(t), t] = \sum_{i=1}^{n} \phi_i[l(t)]\,\phi_i(x_{\mathrm{a}}) \int_0^t f_{\mathrm{a}}(\tau)\, g_i(t-\tau)\,\mathrm{d}\tau \tag{5.8}$$

where n is the number of modes that are measured in discrete measurements of w by the TCSLDV system, which is finite since F_{sa} is finite. The number of virtual measurement points N on the scan path $r(t)$ is determined by $N = F_{\mathrm{sa}}/F_{\mathrm{sc}}$ where F_{sc} is equal to the number of complete scans in 1 s. Multiple series of discrete measurements of w in Eq. (5.8) are formed by lifting them in the lifting method [9]. Each lifted w series corresponds to a virtual measurement point as if it were measured by a transducer attached to the rotating structure at that point. Note that N should be an integer since the laser spot needs to arrive at the same virtual points in each complete scan period; thus F_{sa} should be an integer multiple of F_{sc}. Therefore one has

$$l(t) = l(t + sT_{\mathrm{sc}}) \tag{5.9}$$

where $s = 0, 1, 2, \ldots$ and $T_{\mathrm{sc}} = 1/F_{\mathrm{sc}}$ is the duration of a complete scan period. A complete scan means that the TCSLDV system sweeps its laser spot back and forth once on the scan path $r(t)$. There is a constant sampling time difference $T_{\mathrm{sa}} = 1/F_{\mathrm{sa}}$ between two neighboring lifted w series, which means the lifted w series are not simultaneously registered by the TCSLDV system. Let measurement of w starts at $t = 0$ in Eq. (5.8) when the laser spot arrives at an endpoint of the scan path $r(t)$; the lifted w at the k-th virtual measurement point on the path $r(t)$ can thus be written as a function of sT_{sc}:

$$w_k^l(sT_{\mathrm{sc}}) = w[(k-1)T_{\mathrm{sa}} + (s-1)T_{\mathrm{sc}}] \tag{5.10}$$

where $k = 0, 1, \ldots K$ and $s = 0, 1, \ldots S$, in which K and S are numbers of measurement points and complete scans, respectively. Equation (5.10) shows that the laser spot arrives at the k-th virtual measurement point when $t = (k-1)T_{\mathrm{sa}} + (s-1)T_{\mathrm{sc}}$ and the sampling frequency of w_k^l is equal to F_{sc}. Let $w_{k_1}^l$ and $w_{k_2}^l$ be lifted w at the k_1-th and k_2-th virtual measurement points on the scan path $r(t)$. It can be shown that the correlation function between $w_{k_1}^l$ and $w_{k_2}^l$ can be expressed by [17, 22]

$$\tilde{R}_{k_1k_2}(T) = R\left[\sum_{j=1}^{n} \tilde{A}_j \phi_{j,k_2} \mathrm{e}^{(-\zeta_j\omega_{n,j}+\mathrm{i}\omega_{d,j})(k_2-k_1)T_{\mathrm{sa}}+(-\zeta_j\omega_{n,j}+\mathrm{i}\omega_{d,j})T}\right] \tag{5.11}$$

where $T = \left(m_{k_2} - m_{k_1}\right) T_{\mathrm{sc}}$, $R[\cdot]$ denotes the real part of a complex variable, $\tilde{A}_j$ is a complex factor, and $i = \sqrt{-1}$. By applying a standard OMA algorithm such as the PolyMAX algorithm [23] to power spectra associated with cross-correlation functions, $\omega_{d,j}$, ζ_j, and $\tilde{A}_j\phi_{j,k_2}\mathrm{e}^{(-\zeta_j\omega_{n,j}+\mathrm{i}\omega_{d,j})(k_2-k_1)T_{\mathrm{sa}}}$ in Eq. (5.11) can be estimated, the first two of which are the j-th damped natural frequency and modal damping ratio of the rotating structure, respectively, and ϕ_{j,k_2} in the third of which is the j-th undamped mode shape the rotating structure. The additional term $\mathrm{e}^{(-\zeta_j\omega_{n,j}+\mathrm{i}\omega_{d,j})(k_2-k_1)T_{\mathrm{sa}}}$ in the expression $\tilde{A}_j\phi_{j,k_2}\mathrm{e}^{(-\zeta_j\omega_{n,j}+\mathrm{i}\omega_{d,j})(k_2-k_1)T_{\mathrm{sa}}}$ can be eliminated to obtain ϕ_{j,k_2} with a scaling factor $\tilde{A}_j$ by multiplying the expression by $\mathrm{e}^{-(-\zeta_j\omega_{n,j}+\mathrm{i}\omega_{d,j})(k_2-k_1)T_{\mathrm{sa}}}$ since $\omega_{d,j}$ and ζ_j have been estimated and $(k_2 - k_1)T_{\mathrm{sa}}$ is known. Modal parameters of the rotating structure estimated are not affected by whether the structure is excited at one or multiple points, as long as the reference and measurement points and at least one excitation point are not nodal points of a mode of the structure of interest. ODSs of a rotating structure with a constant or time-varying speed can be estimated by analyzing correlation functions in Eq. (5.11) using the ODS module in the LMS Test.Lab software.

5.3 Experimental Setup

The TCSLDV system was developed in this work for measuring vibration of a rotating structure, and a fan blade with a rotating diameter of 139 cm was used as the rotating structure. The TCSLDV system consists of a Polytec OFV-533 laser Doppler vibrometer, a Cambridge 6240H scanner with an NI 9149 controller, and a Basler camera whose maximum frame rate was 50 Hz (Fig. 5.3a). The controller was connected to the scanner to control rotation angles of two orthogonal mirrors of the scanner. Since the laser beam of the vibrometer was reflected by the mirrors, horizontal and vertical positions of the laser spot on the structure could be controlled by changing rotation angles of X- and Y-mirrors, respectively. A control scheme was designed using the system engineering software LabVIEW so that various scan paths of the laser spot could be created by sending control signals to the scanner. The camera was used to capture images of the rotating fan in Fig. 5.3b with a frame rate of 50 frames per second. Since the TCSLDV system swept its laser spot from one end of the scan path to its other end, which was half of a complete scan, when the camera captured an image of the rotating fan, the number of complete scans in 1 s was half of the frame rate of the camera; therefore $F_{\mathrm{sc}} = 1/2 \times 50 = 25$ Hz. The scan frequency of the TCSLDV system could not exceed 25 Hz since the maximum frame rate of the camera was 50 frames per second, which means Nyquist frequency of the TCSLDV system was 12.5 Hz.

A black circular mark was attached to one blade of the rotating fan so that the TCSLDV system could track the position of the blade by determining the position of the mark. Lower left corners of images captured by the camera were used as references to determine the position of the black circular mark. Every time when the camera captured an image of a rotating fan blade, the image was processed by the LabVIEW software to determine the position of the mark on the blade. Images captured were converted to grayscale images by IMAQ Vision in LabView. IMAQ Find Circular Edge VI in IMAQ Vision could analyze the grayscale images and easily find the position of the black circular mark since it was the only circular item in the images. Since the surface of the blade was white while the mark was black, locations of the mark could be easily

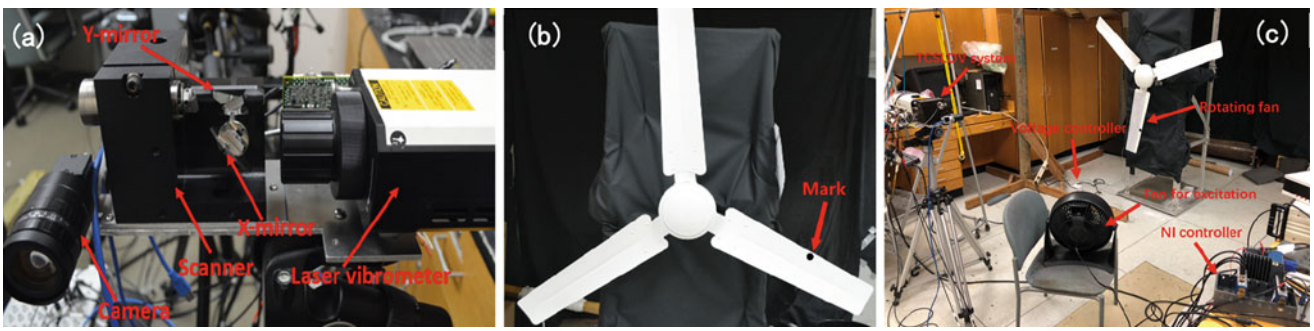

Fig. 5.3 Pictures of (**a**) the TCSLDV system for rotating structure vibration measurement, (**b**) the fan whose blade with a mark is tracked by the camera, and (**c**) the experimental setup

identified in these grayscale images. Since the mark was fixed on the rotating fan blade, the position of the blade could be determined as long as the position of the mark was determined. The controller could control the scanner to track the rotating fan blade and sweep its laser spot along it as the camera continuously captured its images (Fig. 5.3c). Every time when the TCSLDV system determined the position of the mark, it could sweep the laser spot from one end of the scan path to its other end. Since the rotating fan was sufficiently far away from the TCSLDV system and rotation angles of X and Y-mirrors were sufficiently small, horizontal and vertical positions of the laser spot could be considered to be linearly related to rotation angles of X- and Y-mirrors, respectively [17]. Feedback signals of the scanner that are registered in the form of voltage were used to indicate rotation angles of X- and Y-mirrors.

5.4 OMA Results

The first damped natural frequencies and modal damping ratios of the rotating fan blade with three different constant speeds are shown in Table 5.1, and the first undamped mode shapes of the rotating fan blade with the three different rotation speeds are shown in Fig. 5.4a. Revolutions per minute (RPM) was used to represent rotation speed. Spatial position on a scan path is denoted by x/L in Fig. 5.4 where x was the distance between the laser spot and end point of the scan path close to the rotation center and L was the length of the scan path. Since Nyquist frequency of the TCSLDV system was 12.5 Hz and the second damped natural frequency of the stationary fan blade measured by a laser vibrometer was about 27 Hz, only the first modal parameters were estimated. Note that to estimate modal parameters of the stationary fan blade, the fan was turned off and the fan blade was excited by the excitation fan in Fig. 5.3c. The fan blade was basically stationary, but slowly swung back and forth a bit about its downward equilibrium position due to fan excitation, and it was scanned by the TCSLDV system. Note also that undamped mode shapes estimated in this work were normalized by dividing their data by their maximum values. It was seen that there was more uncertainty in damping ratio measurement than damped natural frequency measurement as there was more uncertainty in damping modeling in Eq. (5.1). Compared with the damping of the stationary blade, there was larger damping when the blade rotates due to additional damping from air flow and friction

Table 5.1 First damped natural frequencies and modal damping ratios of the stationary fan blade and the rotating fan blade with three different constant speeds

RPM	Damped natural frequency (Hz)	Modal damping ratio (%)
Stationary	6.22	0.351
9.16 rpm	6.34	0.789
14.25 rpm	6.50	0.709
20.61 rpm	6.73	0.939

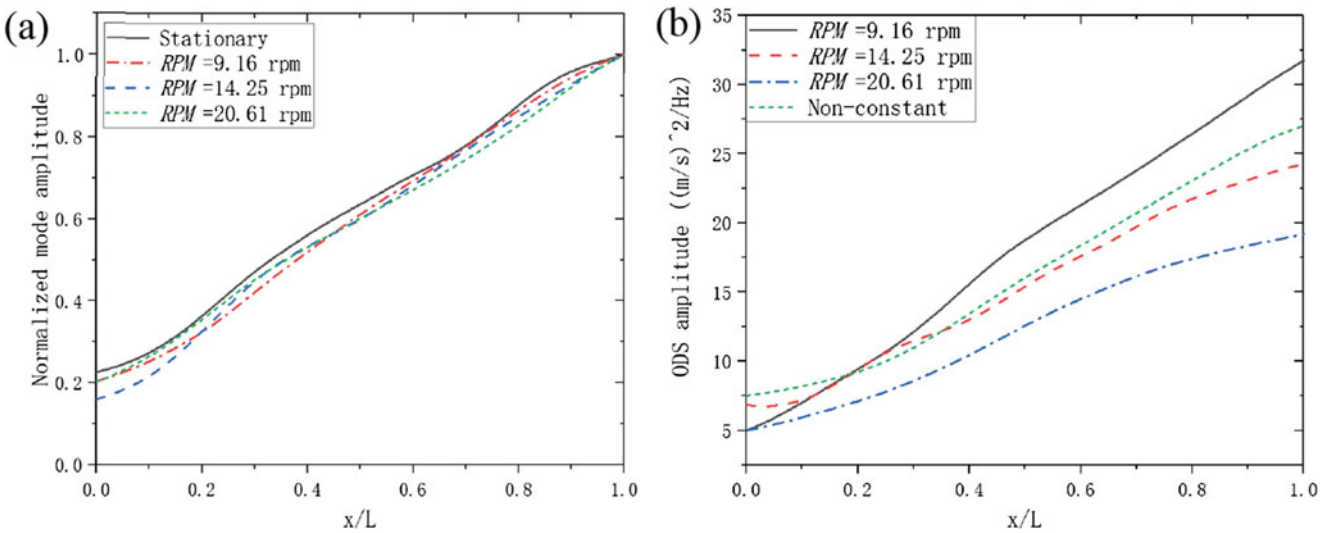

Fig. 5.4 (**a**) First normalized undamped mode shapes of the stationary fan blade and the rotating fan blade with three different constant speeds, and (**b**) ODSs of the rotating fan blade with three different constant speeds and a non-constant speed

damping in the fan motor. Therefore estimated modal damping ratios of rotating fan blade in Table 5.1 were larger than those of stationary fan blade. The estimated first damped natural frequency of the rotating fan blade increases with its speed due to the centrifugal stiffening effect. Estimated ODSs of the rotating fan blade in four tests with three different constant speeds and a non-constant speed are shown in Fig. 5.4b. The estimated ODS of the rotating fan blade with the non-constant speed had a similar shape to those of the rotating fan blade with constant speeds. Differences among ODSs of the rotating fan blade with different speeds in Fig. 5.4b were more pronounced than those among its first normalized undamped mode shapes in Fig. 5.4a, since ODSs depended on wind loads applied on the rotating fan blade and wind loads depended on its rotation speeds, while first normalized undamped mode shapes did not depend on wind loads.

5.5 Conclusion

A novel TCSLDV system was developed to track and scan a rotating structure, and a new OMA method based on a rotating beam vibration theory, an image processing method, and the lifting method is proposed to measure and estimate its modal parameters for a constant rotation speed and ODSs for constant and non-constant rotation speeds. The image processing method determines real-time positions of the rotating structure to calculate its speed and generate a scan path on the structure. The lifting method is used to transform TCSLDV measurement into measurements at multiple virtual measurement points. Correlation functions with non-negative time delays among lifted measurements are calculated and analyzed to estimate modal parameters and ODSs of the rotating structure. Modal parameters a rotating fan blade with a constant speed and ODSs of the fan blade with constant and non-constant speeds are successfully estimated using the new OMA method. A high-speed camera is needed to estimate modal parameters of a rotating structure with high natural frequencies using this OMA method. It is experimentally shown that estimated damped natural frequencies of the rotating fan blade increased with its speed.

Acknowledgments The authors are grateful for the financial support from the National Science Foundation through Grant No. CMMI-1763024. The authors would like to thank Daming Chen for some valuable discussion on the TCSLDV system.

References

1. Ewins, D.J.: Modal Testing: Theory, Practice and Application, 2nd edn. Research Studies Press, Hertfordshire, UK (2000)
2. Xu, Y.F., Zhu, W.D.: Efficient and accurate calculation of discrete frequency response functions and impulse response functions. J. Vib. Acoust. **138**(3), 031003 (2016)
3. Xu, Y.F., Liu, J., Zhu, W.D.: Accurate and efficient calculation of discrete correlation functions and power spectra. J. Sound Vib. **347**, 246–265 (2015)
4. James, G., Carne, T.G., Lauffer, J.P.: The natural excitation technique (NExT) for modal parameter extraction from operating structures. Modal Anal. **10**(4), 260–277 (1995)
5. Siringoringo, D.M., Fujino, Y.: Noncontact operational modal analysis of structural members by laser Doppler vibrometer. Comput. Aided Civ. Inf. Eng. **24**(4), 249–265 (2009)
6. Rothberg, S., Allen, M., Castellini, P.: An international review of laser Doppler vibrometry: Making light work of vibration measurement. Opt. Lasers Eng. **99**(1), 11–22 (2017)
7. Chen, D.M., Xu, Y.F., Zhu, W.D.: Damage identification of beams using a continuously scanning laser Doppler vibrometer system. J. Vib. Acoust. **138**(5), 05011 (2016)
8. Stanbridge, A., Ewins, D.: Modal testing using a scanning laser Doppler vibrometer. Mech. Syst. Signal Process. **13**(2), 255–270 (1999)
9. Allen, M.S., Sracic, M.W.: A new method for processing impact excited continuous-scan laser Doppler vibrometer measurements. Mech. Syst. Signal Process. **24**(3), 721–735 (2010)
10. Stanbridge, A., Ewins, D., Khan, A.: Modal testing using impact excitation and a scanning LDV. Shock. Vib. **7**(2), 91–100 (2000)
11. Chen, D.M., Xu, Y.F., Zhu, W.D.: Experimental investigation of notch-type damage identification with a curvature-based method by using a continuously scanning laser Doppler vibrometer system. J. Nondestruct. Eval. **36**, 38 (2017)
12. Chen, D.M., Xu, Y.F., Zhu, W.D.: Identification of damage in plates using full-field measurement with a continuously scanning laser Doppler vibrometer system. J. Sound Vib. **422**, 542–567 (2018)
13. Xu, Y.F., Chen, D.M., Zhu, W.D.: Damage identification of beam structures using free response shapes obtained by use of a continuously scanning laser Doppler vibrometer system. Mech. Syst. Signal Process. **92**, 226–247 (2017)
14. Yang, S., Allen, M.S.: Output-only modal analysis using continuous-scan laser Doppler vibrometry and application to a 20kw wind turbine. Mech. Syst. Signal Process. **31**, 228–245 (2012)
15. Wereley, N.M., Hall, S.R.: Frequency response of linear time periodic systems. In: 29th IEEE Conference on Decision and Control, Honolulu, HI, USA, vol. 6, pp. 3650–3655 (1990)
16. Yang, S., Allen, M.S.: Lifting approach to simplify output-only continuous-scan laser vibrometry. Mech. Syst. Signal Process. **45**(2), 267–282 (2014)

17. Xu, Y.F., Chen, D.M., Zhu, W.D.: Operational modal analysis using lifted continuously scanning laser Doppler vibrometer measurements and its application to baseline-free structural damage identification. J. Vib. Control. **25**(7), 1341–1364 (2019)
18. Gasparoni, A., Allen, M., Yang, S., Sracic, M., Castellini, P., Tomasini, E.: Experimental modal analysis on a rotating fan using tracking-CSLDV. In: AIP Conference Proceedings, vol. 60, (2010). https://doi.org/10.1063/1.3455482
19. Khalil, H., Kim, D., Nam, J., Park, K.: Operational deflection shape of rotating object using tracking laser Doppler vibrometer. In: 2015 IEEE International Conference on Electronics, Circuits, and Systems (ICECS), Cairo, pp. 693–696 (2015)
20. Zhu, W.D., Mote Jr., C.D.: Dynamic modeling and optimal control of rotating Euler-Bernoulli beams. ASME. J. Dyn. Syst. Meas. Control. **119**(4), 802–808 (1997)
21. Meirovitch, L.: Analytical Methods in Vibrations. The Macmillan Co, New York (1967)
22. Papoulis, A., Pillai, S.U.: Probability, Random Variables, and Stochastic Processes. Tata McGraw-Hill Education, New Delhi (2002)
23. Peeters, B., Van der Auweraer, H., Guillaume, P., Leuridan, J.: The PolyMAX frequency-domain method: A new standard for modal parameter estimation laser. Shock. Vib. **11**(3–4), 395–409 (2004)